Magnetic Resonance in Medicine 50:599–607 (2003)

Arterial Transit Time Imaging With Flow Encoding Arterial Spin Tagging (FEAST)

Jiongjiong Wang,[1,2*] David C. Alsop,[3] Hee Kwon Song,[1] Joseph A. Maldjian,[4] Kathy Tang,[2] Alana E. Salvucci,[2] and John A. Detre[1,2]

Arterial spin labeling (ASL) perfusion imaging provides direct and absolute measurement of cerebral blood flow (CBF). Arterial transit time is a related physiological parameter reflecting the duration for the labeled spins to reach the brain region of interest. Most of the existing ASL approaches to assess arterial transit time rely on multiple measurements at various postlabeling delay times, and thus are vulnerable to motion artifact as well as computational error. We describe the use of flow encoding arterial spin tagging (FEAST) technique to measure tissue transit time, which can be derived from the ratio between the ASL signals measured with and without appropriate bipolar gradients. In the present study, we provided a theoretical framework and carried out an experimental validation during steady-state imaging. The global mean tissue transit time was ~1100 and 1400 ms for two conditions of bipolar gradients with specific encoding velocity (Venc) of 29 and 8 mm/sec, respectively. The mean tissue transit time measured within cerebral vascular territories was shortest in the deep middle cerebral artery (MCA) territory. Application of the FEAST technique in two patients with cerebrovascular disease demonstrated prolonged tissue transit times in the affected vascular territories which were consistent with results from other MR imaging modalities. Magn Reson Med 50:599–607, 2003. © 2003 Wiley-Liss, Inc.

Key words: arterial spin labeling (ASL); cerebral blood flow (CBF); tissue transit time; flow encoding arterial spin tagging (FEAST); functional brain imaging

Arterial transit time is a potentially important physiologic parameter that may reflect the status of hemodynamic impairment in cerebrovascular disease (1). It can be measured using the bolus arrival time of a vascular contrast agent (2). However, absolute measures of cerebral blood flow (CBF) remain challenging in the bolus tracking approach (3,4). Arterial spin labeling (ASL) techniques provide an alternative approach for direct and absolute perfusion quantification using arterial blood water as an endogenous tracer (5,6). ASL is a more economical and less invasive approach compared to exogenous contrast agent methods. While CBF measurements using ASL have been proven reliable in various cerebrovascular and psychiatric disorders (7–9), information regarding arterial transit time is generally not specifically available in ASL methods, although dynamic imaging at varying postlabeling delays has been proposed (10–12). Indeed, arterial transit time has been a major confounding effect in ASL perfusion imaging since in humans the tracer decay rate determined by the T_1 of blood is comparable with arterial transit time (5,6). A considerable amount of effort in developing ASL techniques has been focused on how to eliminate or minimize transit time-related artifacts, including applying a delay time after spin labeling (13) and employing bipolar gradients to spoil the vascular signal (14). However, ASL perfusion MRI may still contain significant transit-related errors even with the use of bipolar gradients or a postlabeling delay (4,7).

Better characterization of the source and significance of transit effects in ASL images would not only help detect potential artifacts in ASL perfusion images, but may also provide valuable diagnostic information that is unavailable with CBF measurements alone. In ASL, arterial transit time is defined as the duration for the tagged blood to flow from the labeling region to the vascular or the tissue compartment of the imaging slices, termed as vascular or tissue transit time, respectively (13). The vascular and tissue transit times are generally considered tightly correlated, with the latter longer than the former. Most existing techniques to assess arterial transit time in ASL rely on multiple measurements of perfusion signals at different postlabeling delay times (10,11,14–17). In normal subjects, shortening of arterial transit time has been found to accompany augmentations in CBF during brain activation (10,11). However, the prohibitively long imaging time to acquire multislice arterial transit time images at different postlabeling delay times limits their potential use in clinical settings and makes the data prone to motion artifacts (4,7).

Here we describe a method termed flow encoding arterial spin tagging (FEAST). This technique can be summarized as a derivation of tissue transit time from the ratio between the perfusion signals in the vascular and microvascular compartments, which are differentiated by appropriate flow encoding bipolar gradients. A similar idea has been mentioned earlier but not systematically addressed (18). In the present study, we provide a theoretical framework and experimental validation during steady-state imaging in normal subjects, along with two case reports demonstrating in patients with cerebrovascular disease.

[1]Department of Radiology, University of Pennsylvania, Philadelphia, Pennsylvania.

[2]Department of Neurology, University of Pennsylvania, Philadelphia, Pennsylvania.

[3]Department of Radiology, Beth Israel Deaconess Medical Center, Harvard Medical School, Boston, Massachusetts.

[4]Department of Neuroradiology, Wake Forest University School of Medicine, Winston-Salem, North Carolina.

Grant sponsor: NIH; Grant numbers: HD39621; DA015149; Grant sponsor: NSF; Grant number: BCS0224007.

*Correspondence to: Jiongjiong Wang, Ph.D., Department of Neurology, University of Pennsylvania, 3400 Spruce Street, Philadelphia, PA 19104. E-mail: jwang@rad.upenn.edu

Received 26 September 2002; revised 5 May 2003; accepted 5 May 2003.

DOI 10.1002/mrm.10559

Published online in Wiley InterScience (www.interscience.wiley.com).

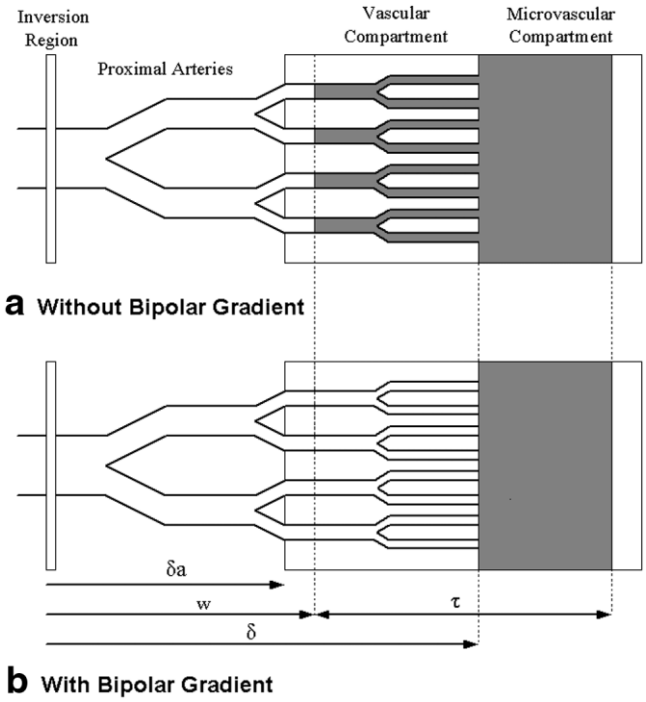

FIG. 1. Diagram of the two-compartment perfusion model and the flow encoding arterial spin tagging (FEAST) technique. In the original ASL technique with a postlabeling delay time (**a**), the perfusion signal acquired without bipolar gradients has two source contributions from the vascular and capillary/tissue compartments. By applying appropriate bipolar gradients to spoil the vascular signal (**b**), only ASL signal in the capillary/tissue compartment is acquired. Tissue transit time can be obtained by the ratio between the ASL signals acquired with and without bipolar gradients. Note that the premise of this model is that the postlabeling delay time is greater than vascular transit time but less than tissue transit time.

THEORY

The FEAST technique is based on the two-compartment perfusion model proposed by Alsop and Detre (13). In their original technique, a delay time was applied between the end of the labeling pulse and the excitation pulse. This postlabeling delay time, w, should ideally be greater than the vascular transit time, δ_a, to allow all of the tagged blood to be delivered into the imaging slices. As displayed in Fig. 1, the raw ASL signal acquired without bipolar gradients, ΔM, consists of two source contributions from the vascular and capillary/tissue compartments, ignoring any outflow of tagged blood through veins. The tissue transit time, δ, is the major factor in determining the proportion of the ASL signal in each of the two compartments, as more tagged blood water resides in the capillary/tissue compartment with shorter tissue transit time and vice versa. Other factors affecting the proportion of ASL signals in the two compartments include the duration of the labeling pulse (τ) and the postlabeling delay time (w). The ASL signal in the capillary/tissue compartment, $\Delta M'$, can be determined by applying appropriate flow encoding bipolar gradients to dampen the vascular ASL signal (14) (see Fig. 1) and the measurements of ΔM and $\Delta M'$ together allow an estimation of the tissue transit time.

We assume that the labeled spins remain primarily in the vasculature and microvasculature rather than exchanging completely with tissue water. In other words, the capillary/tissue compartment can be replaced by the microvascular (capillary) compartment. Given the small difference between the T_1s of blood and brain tissue, this simplified model is quite reasonable, particularly in patients with cerebrovascular disease in whom the arterial transit time may be prolonged (9). The effect of ignoring the T_1 difference between the blood and tissue as well as the different magnetization transfer effect on blood and tissue will be discussed below. For $\delta_a < w < \delta$, the ASL signal measured without and with bipolar gradients can be expressed by the following respective equations (19)

$$\Delta M = \frac{2M_0 f\alpha}{\lambda R_{1a}} [\exp(-wR_{1a}) - \exp(-(\tau + w)R_{1a})] \quad [1]$$

$$\Delta M' = \frac{2M_0 f\alpha}{\lambda R_{1a}} [\exp(-\delta R_{1a}) - \exp(-(\tau + w)R_{1a})] \quad [2]$$

where f is CBF, R_{1a} is the longitudinal relaxation rate of blood, M_0 is the equilibrium magnetization of brain, α is the tagging efficiency, and λ is blood/tissue water partition coefficient. Figure 2a displays the simulation results of the fractional ASL signals acquired with and without bipolar gradients as a function of delay time (w) under conditions of different assumed tissue transit times (δ). The assumed parameters for simulation are $R_{1a} = 0.83$ sec^{-1}, $\alpha = 0.71$, $\lambda = 0.9$ g/ml, and $f = 70$ ml / 100 g/min. In FEAST, the total duration of the labeling pulse and postlabeling delay is constant ($\tau + w = 3.5$ sec), which is defined by TR minus the image acquisition time (see Materials and Methods). One observation in Fig. 2a is that ΔM does not vary at different tissue transit times, which implies that the total ASL signal remains the same no matter what percentage of the tagged blood resides in the vascular or the microvascular (capillary) compartment. Another interesting observation is that, for a given tissue transit time, $\Delta M'$ is a constant irrespective of the delay time (w), assuming ($\tau + w$) is constant. Modulation of w has no effect on the microvascular ASL signal as long as $w < \delta$ (see Fig. 1).

The tissue transit time can be deduced from Eqs. [1] and [2], given the known imaging parameters of w and τ. Figure 2b displays the contour map of the ratio between $\Delta M'$ and ΔM as a function of the delay time (w) at different assumed tissue transit times. It can be seen in Fig. 2b that the ratio approaches 1 when w approaches δ, because most of the labeled blood water has passed through the vascular compartment into the microvasculature. The contour map also shows that longer tissue transit time is associated with smaller ratio of $\Delta M'$ and ΔM.

MATERIALS AND METHODS

Imaging Sequence

The FEAST pulse sequence was based on the CASL technique reported by Alsop and Detre (20). CASL was performed with a 0.25 G/cm gradient and 35 mG RF irradiation applied 8 cm beneath the center of the acquired slices. Controlling for off-resonance artifacts was effected by ap-

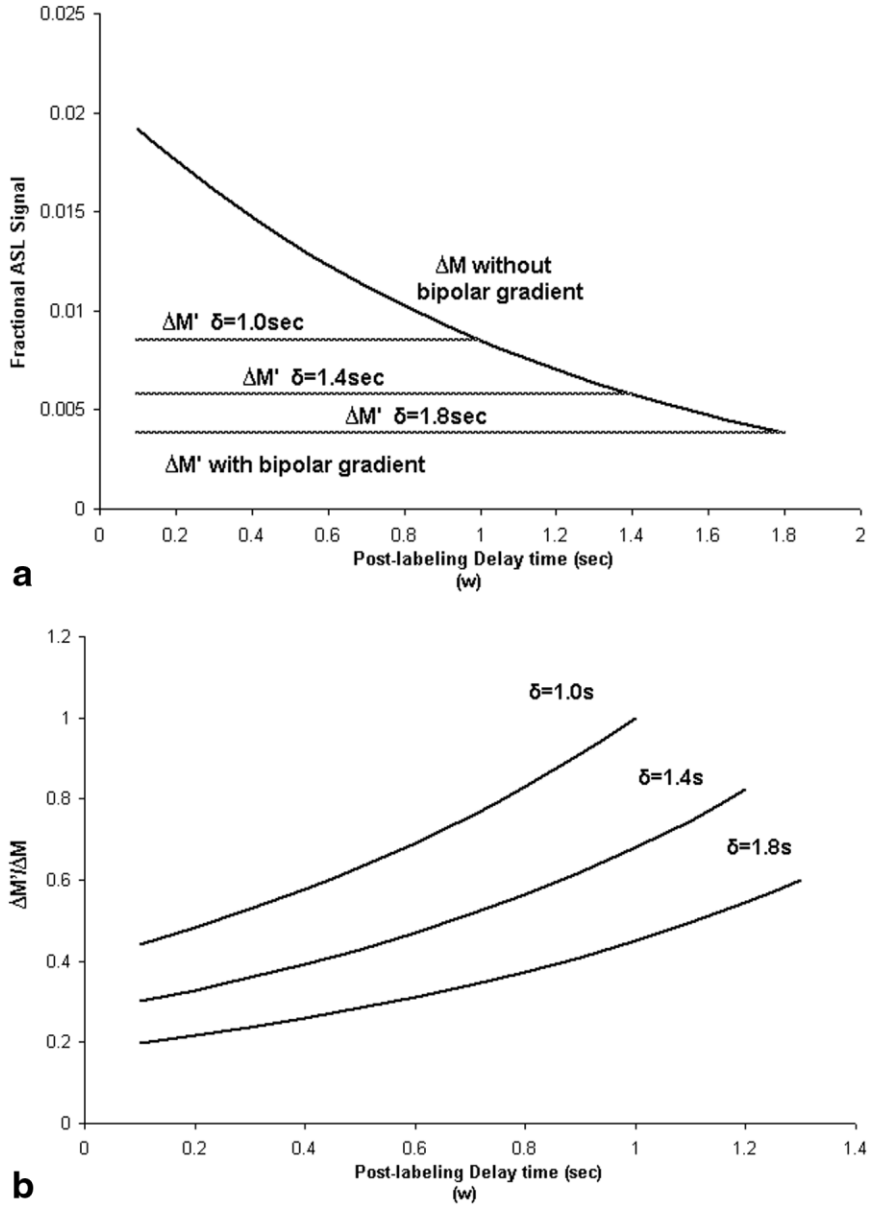

FIG. 2. Theoretical calculation based on Eqs. [1] and [2] showing (**a**) the fractional ASL signals (ΔM and $\Delta M'$) as a function of postlabeling delay time under conditions of different tissue transit times; (**b**) the contour map of the ratio between $\Delta M'$ and ΔM as a function of the postlabeling delay time at various tissue transit times. In the simulation, f is assumed to be 70 ml / 100 g/min, tagging efficiency is 0.71, and blood T_1 is 1.2 sec.

plying an amplitude modulated version of the labeling pulse based on a sinusoid function with a modulation frequency of 125 Hz and amplitude of 49.5 mG. Interleaved images with labeling and control pulses were acquired using a single-shot gradient-echo blipped echo-planer imaging (EPI) sequence. A pair of bipolar gradients was placed between the excitation pulse and EPI acquisition along the slice direction, with no gap between the positive and negative lobes. The amplitude of the bipolar gradients was set to 0 for odd pair of label and control acquisitions and 2.1 G/cm for even pair of label and control acquisitions. This interleaved acquisition minimized the effects of motion between the ASL data with and without bipolar gradients to avoid systematic errors in flow due to gradual changes in physiological state.

Imaging parameters were: FOV = 24 × 16 cm, 64 × 40 matrix, TR = 4 sec, bandwidth 62.5 kHz, slice thickness 14 mm, interslice space 2 mm. Five axial slices were acquired sequentially from inferior to superior to cover most of the supratentorial brain and each slice acquisition took about 80 ms. Each acquisition of the FEAST sequence consisted of the labeling (control) pulse, postlabeling delay, and EPI image acquisition. The duration of the labeling irradiation (τ) was set to be the difference between the repetition time (TR) and the delay time (w) plus the image acquisition time. For example, with a fixed TR of 4 sec the labeling pulse was applied for 2.3 sec when w = 1.2 sec and 2.9 sec when w = 0.6 sec (20). Both the postlabeling delay and the width of the bipolar gradients were systematically varied during the experiments while holding TR constant.

MR Scanning

Imaging was performed on a 1.5T whole-body scanner (GE Medical Systems, Milwaukee, WI) with the product

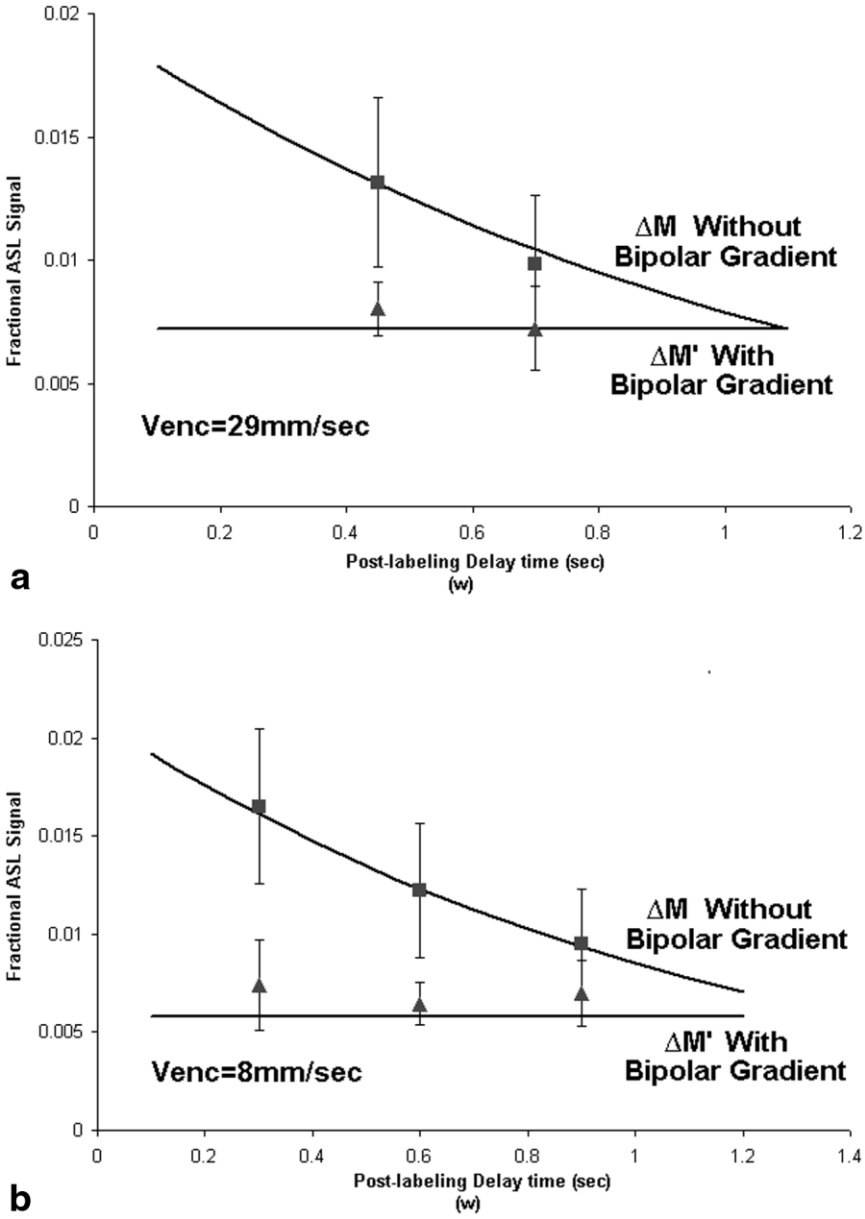

FIG. 3. The mean fractional ASL signals measured within the gray matter ROIs using bipolar gradients with 4 ms (**a**) and 8 ms (**b**) pulse width, respectively. Square and triangle symbols represent ASL signals acquired without and with bipolar gradients, respectively. Error bars indicate standard deviation. Simulated curves are based on Eqs. [1] and [2] with assumed tissue transit time of 1100 (**a**) and 1400 ms (**b**). Fitted CBF values are ~70 (**a**) and 65 ml / 100 g/min (**b**), respectively. The ASL signal acquired without bipolar gradients decays exponentially with the T_1 of blood while the ASL signal acquired with bipolar gradients remains constant at different postlabeling delay times.

quadrature head coil. Written informed consent was obtained prior to all human studies according to a protocol approved by the University of Pennsylvania Institutional Review Board. MR scanning was performed on 14 healthy subjects (nine males, five females, age 22–38 years, mean 28.1 years) and two patients with cerebrovascular disease (30 years and 82 years, female).

One critical point in carrying out the FEAST technique is the choice of appropriate amplitude and width of the bipolar gradients to spoil coherently flowing spins inside the vessels. The typical blood flow velocity in the capillaries is on the order of a few millimeters per second (21,22), therefore the bipolar gradient should have a specific encoding velocity (Venc) just above that range. According to this physiological criteria, bipolar gradients with 8 ms pulse width (for each positive/negative pulse) were chosen in the present study, corresponding to Venc of 8 mm/sec and b value of 11 sec/mm^2. On the other hand, strong gradients might lead to penalties in signal-to-noise ratio (SNR) by spoiling the vascular ASL signal. We also examined experimental conditions using bipolar gradients with 4 ms pulse width, corresponding to a Venc of 29 mm/sec and b value of 2 sec/mm^2. The TE was 39 ms and 31 ms for two conditions of 8 ms and 4 ms width bipolar gradients, respectively (same for acquisitions with and without bipolar gradients). It was expected that the tissue transit time measured using the bipolar gradients of 4 ms width would be shorter than that measured with bipolar gradients of 8 ms width.

The delay time (w) in the current experiments was systematically varied in order to verify the perfusion model described in Eqs. [1] and [2]. Eight of the total 14 healthy subjects were scanned using the long width bipolar gradients at three postlabeling delay times of 300, 600, and 900 ms, while the other six subjects underwent scans using the short width bipolar gradients at two postlabeling

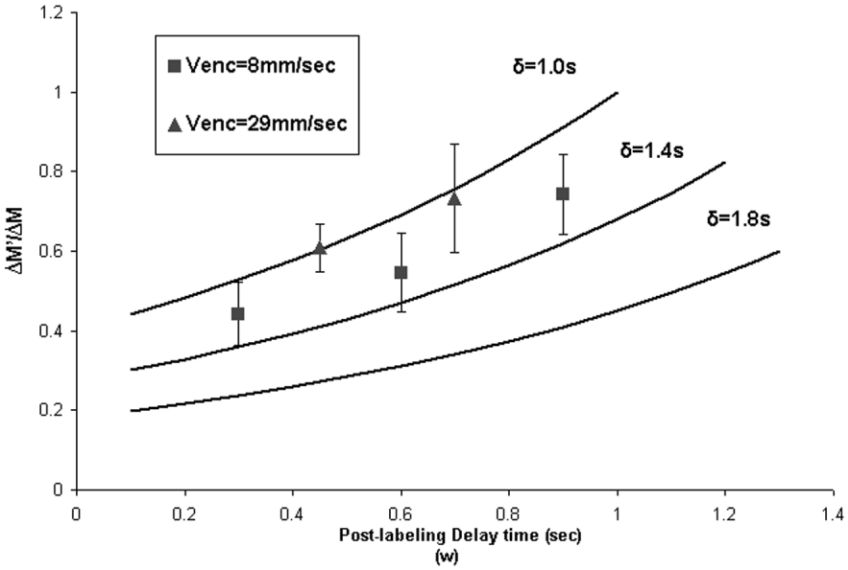

FIG. 4. The mean ratio ($\Delta M'/\Delta M$) between ASL signals acquired with and without bipolar gradients as a function of the postlabeling delay time; the experimental results are overlaid upon the simulation results as in Fig. 2b. Square and triangle symbols represent the measured ratio with 8 ms and 4 ms width gradients, respectively. Error bars indicate standard deviation.

delay times of 450 and 700 ms. The order of the scans at different postlabeling delay times was counterbalanced across subjects to avoid systematic error. Each scan at a particular postlabeling delay time consisted of 120 acquisitions with a scan time of 8 min, corresponding to 30 pairs of label and control acquisitions with bipolar gradients on and off, respectively. "Dummy" gradient and RF pulses preceded each scan to allow tissue to reach steady-state magnetization. A 3D inversion prepared spoiled GRASS sequence was used for T_1-weighted anatomical images.

Data Processing

Data were reconstructed offline and corrected for geometric distortion (23). The raw images in each scan acquired at a particular postlabeling delay time were separated into label and control pairs and then pair-wise subtracted. The difference images for ASL with (even number) and without (odd number) bipolar gradient were separated, corrected for motion and physiological fluctuation using an algorithm based on principal component analysis (24), followed by averaging across the image series to form two mean ASL perfusion images (ΔM and $\Delta M'$). Images of the tissue transit time (δ) were then calculated based on Eqs. [1] and [2] and the ΔM, $\Delta M'$ images were spatially smoothed with a 2D 1.5 voxel Gaussian kernel.

SPM99 software was used to segment the T_1-weighted anatomical images into three whole brain regions of interest (ROIs) of gray, white matter, and cerebrospinal fluid. The mean tissue transit time, ΔM and $\Delta M'$, along with the raw image intensity were measured within the gray matter ROIs (white matter ROIs were not used due to the low ASL signal which may be very sensitive to noise). Subsequently, segmentation of tissue transit time images into major vascular territories was performed using an automated ROI analysis based on published templates (25) following data transformation into Talairach space using T_1-weighted anatomical images. The vascular territories studied included deep anterior cerebral artery (ACA), deep middle cerebral artery (MCA), leptomeningeal ACA, MCA, and posterior cerebral artery (PCA) territories in the left and right brain hemispheres, respectively (see template figs. in (9)). The ROI-based measurements of tissue transit time were analyzed using repeated-measures ANOVA in the SPSS (Chicago, IL) software package to compare findings in different territories.

Patient Scans

The FEAST sequence with 8 ms pulse width bipolar gradients was performed on two patients with cerebrovascular disease: one stroke patient (30 years, female) and another diagnosed with left internal carotid artery (ICA) and MCA stenosis (82 years, female). A single postlabeling delay time of 800 ms was used and the acquisition number was 180 to improve the SNR. Fluid-attenuation inversion recovery (FLAIR) images and diffusion-weighted images (DWI) were obtained on the patient, along with a "standard" CASL perfusion MRI using a postlabeling delay time of 1500 ms (7). For the CASL scan, 8 slices (8 mm thick and 2 mm gap) were acquired from inferior to superior in an interleaved order using 90 acquisitions.

RESULTS

Figure 3a,b displays the mean fractional ASL signals (ΔM and $\Delta M'$) measured within the gray matter ROIs using 4 ms and 8 ms pulse width bipolar gradients, respectively. The solid lines are the simulated curves based on Eqs. [1] and [2], with assumed tissue transit times (δ) of 1100 and 1400 ms, respectively (see below). Fitting the above model with the experimental data yields CBF values of 70 and 65 ml / 100 g/min in Fig. 3a,b, respectively. It can be clearly seen that the experimental results match well with the theoretical model: the ASL signal acquired without bipolar gradients decays exponentially with the T_1 of blood, while the ASL signal acquired with bipolar gradients remains constant at different postlabeling delay times. Figure 4 illustrates the mean ratio between ASL signals

Table 1
Mean Tissue Transit Time Averaged Across Subjects at Different Postlabeling Delay Times

Postlabeling Delay time	Venc = 8mm/sec (n = 8)			Venc = 29mm/sec (n = 6)	
	300 ms	600 ms	900 ms	450 ms	700 ms
Tissue transit time Mean ± SD (ms)	1323.2 ±209.0	1432.9 ±177.5	1393.4 ±116.7	1116.0 ±147.0	1148.6 ±232.3

acquired with and without bipolar gradients ($\Delta M'/\Delta M$) as a function of the postlabeling delay time. The experimental results are overlaid upon the simulation results from Fig. 2b. The measured data points align well with the simulated contour curves. As seen in Table 1, the experimental values for the tissue transit time are very similar at different postlabeling delay times, but are shorter using the 4 ms width bipolar gradients (~1100 ms) compared to the 8 ms width gradients (~1400 ms). The difference between the two measures of mean tissue transit time is statistically significant ($P = 0.016$, unpaired two-tailed t-test).

Figure 5 shows the mean tissue transit times based on cerebral vascular territories averaged across subjects and different postlabeling delay times. The measures of the tissue transit time under two bipolar gradient strengths show similar patterns of variation across vascular territories, with the shortest values in the deep left and right MCA territories. This result is consistent with the neuroanatomy of cerebral blood supply since the deep MCA branches are closest to the internal carotid artery (26). The repeated-measures ANOVA analysis indicates that the main effect of vascular territory is significant for data acquired using the 8 ms bipolar gradients ($F(4,4) = 45.9$, $P = 0.005$), but only displays a trend for the data acquired using the 4ms gradients ($F(4,2) = 3.69$, $P = 0.225$). As can also be seen in Fig. 5, the global tissue transit time measured using 4 ms width bipolar gradients is much shorter than that measured using 8 ms width gradients. No statistical significance is found for the effects of postlabeling delay time and brain hemisphere.

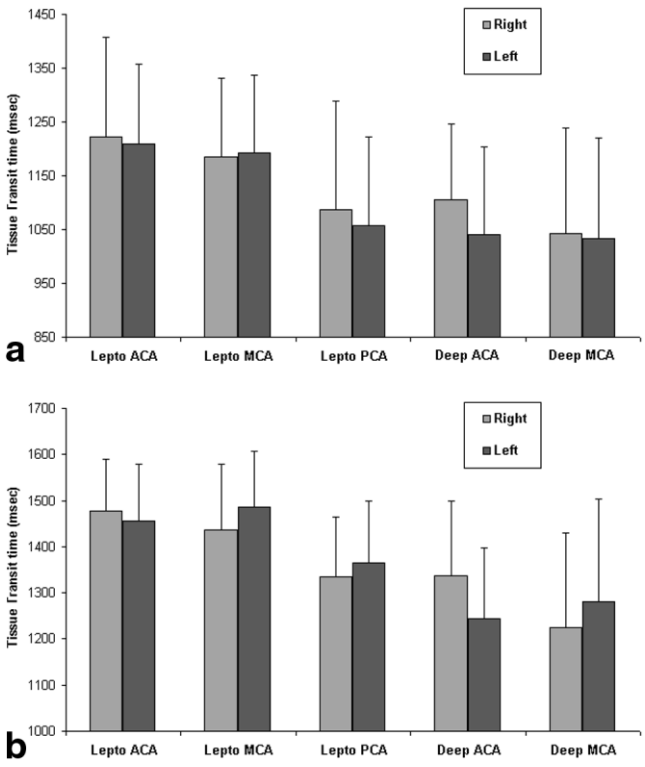

FIG. 5. Column plots of the mean tissue transit time based on cerebral vascular territories averaged across subjects and different postlabeling delay times. The measures of the tissue transit time with 4 ms (**a**) and 8 ms (**b**) width bipolar gradients show very similar patterns of variation across vascular territories, with the shortest tissue transit time in the deep left and right MCA territories. Error bars indicate standard deviation.

Figure 6a,b displays ASL difference perfusion images and the corresponding tissue transit time images from two representative subjects for 4 ms and 8 ms bipolar gradients. The ASL perfusion images show decreased intensity of ΔM with prolonged delay time (w) while the microvascular $\Delta M'$ signals remain roughly unchanged, consistent with theoretical and experimental results displayed in Fig. 3. By visual inspection of the $\Delta M'$ images, most of the focal bright intravascular signals have been "spoiled" by the 8 ms width bipolar gradients in Fig. 6b, whereas noticeable intravascular signals still exist with the 4 ms width gradients in Fig. 6a. The tissue transit time images are generally uniform in gray matter regions and the measured values are quite consistent across different postlabeling delay times. Variation in the measurements of tissue transit time is observed across postlabeling delay times in the white matter areas, where perfusion SNR is marginal. Interestingly, even with a short postlabeling delay time of 300 ms the tissue transit time images show comparable quality and quantity with those acquired at longer postlabeling delay times. This phenomenon, along with the data shown in Fig. 3b, suggests that the vascular transit time (δ_a) for the tagged blood to reach imaging voxels is relatively short in normal subjects and is a less important physiological parameter as compared with tissue transit time (δ).

Results obtained from a patient with subacute stroke are displayed in Fig. 7, showing four slices relevant to the deficit. The patient was scanned ~2 weeks from the onset of stroke symptoms. Both the DWI and FLAIR images show infarcts in the patient's left MCA territory. The CASL CBF images display areas of focal hyperintensity within a larger area of hypointensity in the corresponding vascular territory. However, quantification of CBF within the MCA territories remains normal or even slightly higher on the left (36.2 ml / 100 g/min) as compared to the right hemisphere (32.5 ml / 100 g/min). As indicated in the FEAST images, almost all the left MCA territory has prolonged tissue transit time (2460 ms vs. 1763 ms in the right MCA territory), suggesting that perfusion in this region is being maintained through collateral blood supply. There are some regions in brain tissue that are not reached by the

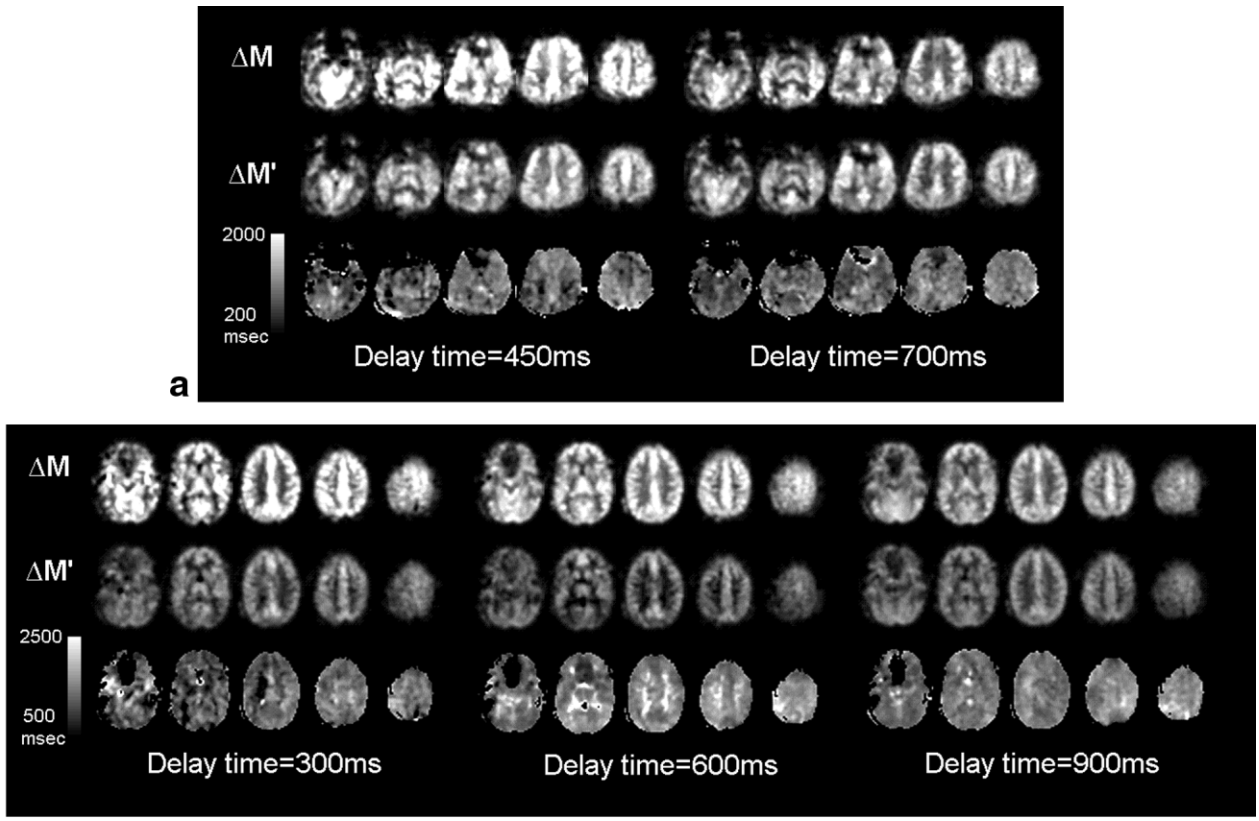

FIG. 6. The ASL difference perfusion images (upper two rows) and the corresponding tissue transit time images (bottom row) of two representative subjects acquired with 4 ms (**a**) and 8 ms (**b**) width bipolar gradients.

tagged blood at the applied postlabeling delay time of 800 ms, where tissue transit time cannot be measured with the parameters used in this study.

Results obtained from a patient with left MCA and ICA stenosis are displayed in Fig. 8, showing CBF, tissue transit time, and MR angiography (MRA) images. The MRA results clearly indicate abnormal narrowing (stenosis) of the left MCA, ICA branches as well as blockage of the left communicating artery (arrows). The CASL CBF images show corresponding widespread focal intravascular signals caused by delayed arterial transit time in the left hemisphere. However, average perfusion measured in the left hemisphere (65.4 ml / 100 g/min) is even higher than perfusion in the right hemisphere (57.2 ml / 100 g/min). Tissue transit time, as indicated in the FEAST images, is prolonged in the whole affected left hemisphere (1644 ms) compared to the normal right side (1168 ms). The tissue transit time results not only explain the transit effects observed in the CASL CBF images, the spatial extent of the deficits also suggests a lesion in the large proximal arteries, which is consistent with the clinical MRA results.

DISCUSSION

The present study demonstrated the feasibility of deriving tissue transit time through interleaved CASL measurements with and without appropriate flow encoding bipolar gradients. The experimental results not only match well with the theoretical model, but also are compatible with arterial transit time values reported in previous studies primarily through multiple measurements, e.g., 0.94 sec by Ye et al. (14); 1.3 sec by Wong et al. (27); 0.6–1.2 sec by Gonzalez-At et al. (11); and 0.73-0.97 sec by Yang et al. (15) (including both vascular and tissue transit times). Compared to approaches relying on multiple measurements by varying the delay time (w) or the labeling pulse duration, the current technique is more time efficient, less sensitive to motion artifacts, and has reduced computational demand since no nonlinear iterative methods are required. Compared to the contrast agent approaches, it has the advantages of being totally noninvasive and the capability for simultaneous quantification of absolute CBF. Potentially, information regarding cerebral blood volume (CBV) could also be estimated from CBF and tissue transit time values. For example, a rough estimation of arterial CBV can be obtained by the product of CBF and δ, yielding $\sim$1.4% arterial blood volume in normal subjects. Note the concept of arterial transit time in ASL is different from the mean transit time in contrast agent approaches which denotes the average duration for a bolus to pass from the arterial to the venous end. Arterial transit time is conceptually similar to the bolus arrival time or the time to peak in contrast agent methods.

A critical factor in the FEAST technique is the choice of appropriate bipolar gradients and postlabeling delay time. As mentioned in Materials and Methods, the Venc of the bipolar gradients should be slightly greater than the typical flow velocities in the capillaries, but practical compro-

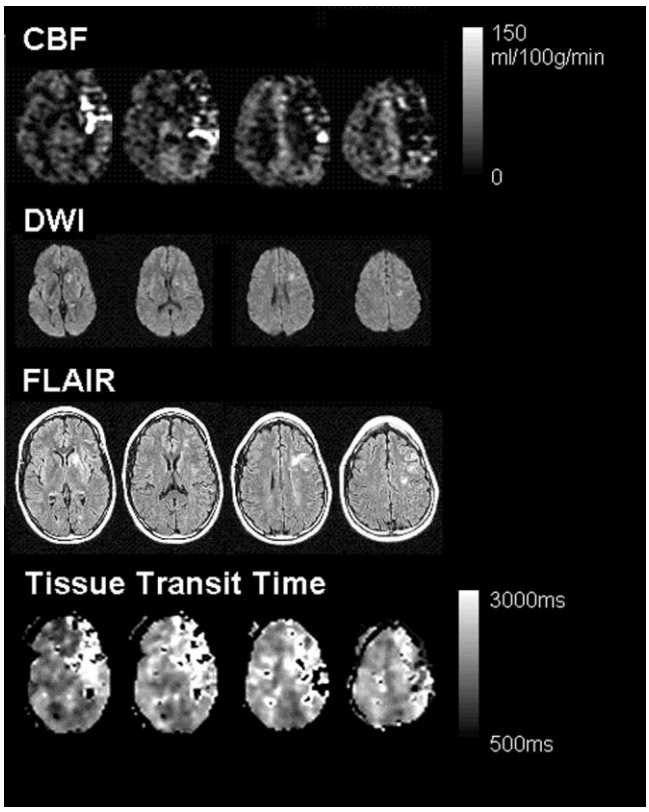

FIG. 7. 30-year-old female patient images including CBF, diffusion weighted (DWI), T_2-weighted (FLAIR), and FEAST tissue transit time images.

mise could be made to ensure adequate SNR and reliability of the tissue transit time measurements. Our results suggest a globally reduced tissue transit time when weaker bipolar gradients are applied; however, the relative spatial distribution of tissue transit time remains largely the same (see Fig. 5). Both gradient pulse durations used in the present study are acceptable, with the 4 ms width gradients being slightly weaker compared to other studies (e.g., Venc of 15 mm/sec, b = 4.5 sec/mm^2 in Ref. 14). Wong et al. (27) used bipolar gradients with a b value of 22 sec/mm^2 and the tissue transit time they measured was 1.3 sec, which is very close to the present results, suggesting there might be little benefit to apply gradients with excessive strength. The choice of the postlabeling delay time depends on the bipolar gradients, since the stronger the bipolar gradients are, the longer the postlabeling delay time can be (see Fig 2a). The postlabeling delay time ideally should be long enough for all the tagged blood to arrive in the imaging slices, but short enough before all the tagged blood enters microvasculature. For parameters used in the current experiments, a range of 400–800 ms seems to be optimal with most bipolar gradient encodings.

The relatively good fit between the experimental data and the simulation results demonstrated in Figs. 3 and 4 suggests that the simplified perfusion model is valid. Ignoring the difference between T_1s of blood and brain tissue could result in potential errors in CBF measurements, e.g., an underestimation of flow in short T_1 tissues, such as white matter, and an overestimation of flow in long T_1 tissues, such as an edematous lesion in the gray matter (9). However, our simulation results demonstrated it is not a severe problem: a T_1 change of 200 ms would result in less than a 10% change in CBF estimation (19), and the error in the measures of tissue transit time is expected to be even less because it depends on the ratio between $\Delta M'$ and ΔM. Another potential source of error is the magnetization transfer effect, which would cause reduced T_1 in the brain tissue. This off-resonance saturation effect is manifested as a signal variation of the raw MR images at different delay times (w). Within the current experimental range of w = 300–900 ms, the raw image intensities measured at different postlabeling delay times showed only about 6% signal variation. Since the ASL signal roughly scales with the raw image intensity, this observation suggests ASL signal variation due to the magnetization transfer effect is relatively small. The major tradeoff of applying the flow encoding bipolar gradients is the loss in SNR. High field ASL should largely circumvent this issue because of the advantages in prolonged blood T_1 and increased SNR (19). A longer postlabeling delay time could be applied at higher magnetic field, which would allow longer tissue transit time to be determined. Bipolar gradients could also be applied along two or three directions to shorten TE and improve the spoiling of the vascular signal. In addition, the current method can also be applied to pulsed ASL (PASL) approaches (18).

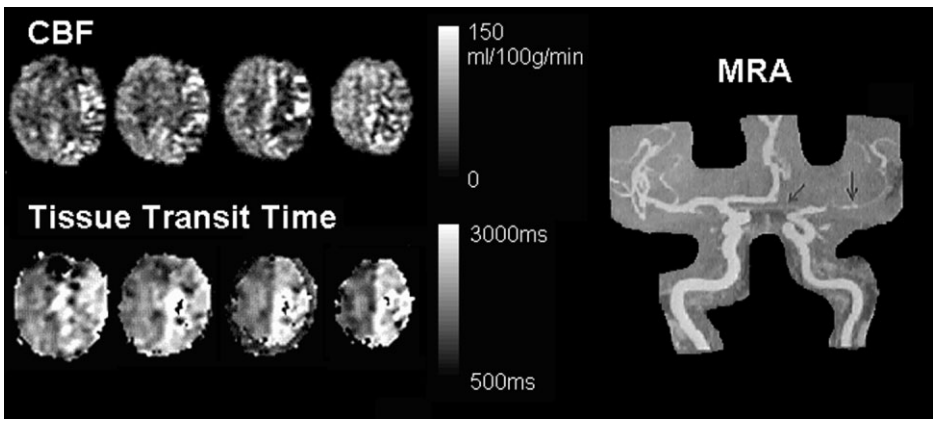

FIG. 8. 82-year-old female patient images including CBF, FEAST tissue transit time images, and MR angiography.

CONCLUSION

A novel noninvasive MR approach to estimate tissue transit time has been introduced. Experimental results and theoretical simulations demonstrate the feasibility of this method. Given its relative insensitivity to motion artifact, superior computational and scan time efficiency, the FEAST technique could be a useful tool in both clinical and neuroscience applications.

ACKNOWLEDGMENTS

The authors thank Dr. Geon-Ho Jahng for help with the manuscript.

REFERENCES

1. Derdeyn CP, Grubb Jr RL, Powers WJ. Cerebral hemodynamic impairment: methods of measurement and association with stroke risk. Neurology 1999;53:251–259.
2. Smith AM, Grandin CB, Duprez T, Mataigne F, Cosnard G. Whole brain quantitative CBF, CBV, and MTT measurements using MRI bolus tracking: implementation and application to data acquired from hyperacute stroke patients. J Magn Reson Imag 2000;12:400–410.
3. McLaughlin AC, Ye FQ, Berman KF, Mattay VS, Frank JA, Weinberger DR. Use of diffusible and nondiffusible tracers in studies of brain perfusion. In: Moonen CTW, Bandettini PA, editors. Functional MRI. Berlin: Springer; 1999.
4. Calamante F, Gadian DG, Connelly A. Quantification of perfusion using bolus tracking magnetic resonance imaging in stroke: assumptions, limitations, and potential implications for clinical use. Stroke 2002;33: 1146–1151.
5. Detre JA, Alsop DC. Perfusion fMRI with arterial spin labeling (ASL). In: Moonen CTW, Bandettini PA, editors. Functional MRI. Heidelberg: Springer; 1999. p 47–62.
6. Wong EC. Potential and pitfalls of arterial spin labeling based perfusion imaging techniques for MRI. In: Moonen CTW, Bandettini PA, editors. Functional MRI. Heidelberg: Springer; 1999. p 63–69.
7. Detre JA, Alsop DC, Vives LR, Maccotta L, Teener JW, Raps EC. Noninvasive MRI evaluation of cerebral blood flow in cerebrovascular disease. Neurology 1998;50:633–641.
8. Alsop DC, Detre JA, Grossman M. Assessment of cerebral blood flow in Alzheimer's disease by spin-labeled magnetic resonance imaging. Ann Neurol 2000;47:93–100.
9. Chalela JA, Alsop DC, Gonzalez-Atavalez JB, Maldjian JA, Kasner SE, Detre JA. Magnetic resonance perfusion imaging in acute ischemic stroke using continuous arterial spin labeling. Stroke 2000;31:680–687.
10. Yang Y, Engelien W, Xu S, Gu H, Silbersweig DA, Stern E. Transit time, trailing time, and cerebral blood flow during brain activation: measurement using multislice, pulsed spin-labeling perfusion imaging. Magn Reson Med 2000;44:680–685.
11. Gonzalez-At JB, Alsop DC, Detre JA. Perfusion and transit time changes during task activation determined with steady-state arterial spin labeling. Magn Reson Med 2000;43:739–746.
12. Gunther M, Bock M, Schad LR. Arterial spin labeling in combination with a Look-Locker sampling strategy: inflow turbo-sampling EPI-FAIR (ITS-FAIR). Magn Reson Med 2001;46:974–984.
13. Alsop DC, Detre JA. Reduced transit-time sensitivity in noninvasive magnetic resonance imaging of human cerebral blood flow. J Cereb Blood Flow Metab 1996;16:1236–1249.
14. Ye FQ, Mattay VS, Jezzard P, Frank JA, Weinberger DR, McLaughlin AC. Correction for vascular artifacts in cerebral blood flow values measured by using arterial spin tagging techniques. Magn Reson Med 1997;37:226–235.
15. Yang Y, Frank JA, Hou L, Ye FQ, McLaughlin AC, Duyn JH. Multislice imaging of quantitative cerebral perfusion with pulsed arterial spin labeling. Magn Reson Med 1998;39:825–832.
16. Figueiredo P, Clare S, Jezzard P. Issues in quantitative perfusion and arterial transit time mapping using pulsed ASL. In: Proc 10th Annual Meeting ISMRM, Honolulu, 2002. p 623.
17. Wong EC, Buxton RB, Frank LR. Implementation of quantitative perfusion imaging techniques for functional brain mapping using pulsed arterial spin labeling. NMR Biomed 1997;10:237–249.
18. Wong EC, Buxton RB, Frank LR. Direct and indirect measurements of the time of exchange of tagged arterial water into brain tissue in pulsed ASL. In: Proc 6th Annual Meeting ISMRM, Sydney, 1998. p 1199.
19. Wang J, Alsop DC, Li L, Listerud J, Gonzalez-At JB, Schnall MD, Detre JA. Comparison of quantitative perfusion imaging using arterial spin labeling at 1.5 and 4 Telsa. Magn Reson Med 2002;48:242–254.
20. Alsop DC, Detre JA. Multisection cerebral blood flow mr imaging with continuous arterial spin labeling. Radiology 1998;208:410–416.
21. Berne RM, Levy MN. Cardiovascular physiology. St. Louis: Mosby-Year Book; 1992.
22. Mchedlishvili G. Arterial behavior and blood circulation in the brain. New York: Plenum Press; 1986.
23. Alsop DC. Correction of ghost artifacts and distortion in echo-planar MR imaging with an iterative reconstruction technique (abstract). Radiology 1995;197P:388.
24. Alsop DC, Detre JA. Reduction of excess noise in fMRI time series data using noise image templates (abstract). In: Proc 5th Annual Meeting ISMRM, Vancouver, 1997. p 1687.
25. Tatu L, Moulin T, Bogousslavsky J, Duvernoy H. Arterial territories of the human brain: cerebral hemispheres. Neurology 1998;50:1699–1708.
26. Carpenter MB. Core text of neuroanatomy. Baltimore: Williams & Wilkins; 1991.
27. Wong EC, Buxton RB, Frank LR. A theoretical and experimental comparison of continuous and pulsed arterial spin labeling techniques for quantitative perfusion imaging. Magn Reson Med 1998;40:348–355.